PHYSICAL REVIEW B VOLUME 36, NUMBER 12 15 OCTOBER 1987-II

Energy-band structure of NbC studied with angle-resolved photoelectron spectroscopy

P. A. P. Lindberg, L. I. Johansson, J. B. Lindström, and P. E. S. Persson
Department of Physics and Measurement Technology, Linköping University, S-581 83 Linköping, Sweden

D. S. L. Law
Science and Engineering Research Council, Daresbury Laboratory, Daresbury, Warrington WA4 4AD, United Kingdom

A. N. Christensen
Department of Chemistry, Aarhus University, DK-8000 Aarhus C, Denmark
(Received 6 February 1987)

The (100) face of $NbC_{0.83}$ has been studied using angle-resolved photoelectron spectroscopy and synchrotron radiation as the excitation source. The experimental results are compared with the theoretical energy-band structure calculated for stoichiometric NbC using the linear augmented-plane-wave method. A good agreement between theory and experiment is found for the main structures in the experimental spectra. The origin of the experimental features that cannot be explained by the calculated energy bands is discussed in terms of surface and vacancy-induced effects. A resonant enhancement of the emission close to the Fermi energy at photon energies above the Nb 4*p* threshold is presented and discussed.

I. INTRODUCTION

The transition-metal nitrides and carbides (TMNC's) possess many scientifically interesting and technologically important properties.[1] On the microscopic level they display three different types of bonding characteristics: metallic, ionic, and covalent. This unusual combination of binding mechanisms manifests itself in their macroscopical properties. They exhibit ultrahardness and high melting points as well as metallic conductivity. These very useful properties are ultimately determined by the electronic structure of the material.

Photoelectron spectroscopy in the ultraviolet photon-energy range (UPS) has proved to be a very powerful tool to investigate the electronic structure of solids.[2] Its surface sensitivity and the possibility of doing **k**-selective measurements make it very suitable for examining surface reactivity and energy-band dispersions. By utilizing synchrotron radiation the full capacity of UPS can be used. The tunability of the radiation allows the dispersion of bulk bands to be mapped out, and in normal emission, surface states can often be sorted out from those of the bulk, since they are not expected to show any dispersion with the photon energy. Moreover, the high degree of polarization of the radiation facilitates identification of the symmetry of the initial states.

In order to interpret the photoemission data a theoretical description of the electronic structure is required. Since TMNC's crystallize in the sodium chloride structure, they are fairly simple to treat theoretically. However, their tendency to have vacancies in the nonmetal sublattice complicates the treatment severely, although during recent years considerable improvements in describing substoichiometric systems theoretically have been made. Density-of-states calculations have been performed for various nonmetal-deficient systems of the TMNC's and very recently it has even become possible to calculate angle-resolved photoemission spectra for TMNC's of different composition.[3,4]

In the case of NbC several theoretical studies[5–12] have increased the understanding of the electronic structure. On the experimental side, there is, however, not so much information available in the literature. Angle-integrated photoemission measurements[13–15] in the UPS as well as in the XPS regime have been performed and a good agreement with the theoretical density of states was found. In the latter work[15] a vacancy-induced structure was revealed in the difference spectra for two compounds of different stoichiometry. However, to our knowledge, there are no angle-resolved measurements reported for NbC. Angle-resolved photoemission measurements provide, in contrast to their angle-integrated counterparts, detailed information about the electronic structure of crystalline solids; the electron energy levels can be probed as a function of the wave vector and different crystal faces can be investigated, or in short, angle-resolved measurements allow the parts to be separated from the whole.

In order to examine the electronic structure of the (100) surface of NbC, we have performed angle-resolved photoemission experiments in the photon energy range 17–65 eV. The results from a linear augmented-plane-wave band-structure calculation performed for stoichiometric NbC are presented and used to analyze the photoemission data. The calculated band structure is found to explain three of the experimental peaks, two of which as due to direct transitions and the third as arising from a one-dimensional density-of-states effect. Experimental features that may be due to vacancy- and surface-induced effects are also reported. At the higher

photon energies a strong enhancement of the emission strength at the Fermi energy is observed and its origin is discussed.

II. EXPERIMENTAL DETAILS

Angle-resolved photoelectron-spectroscopy measurements have been performed utilizing synchrotron radiation on beam line 6.2, at the Daresbury Synchrotron Radiation Source, which is equipped with a toroidal-grating monochromator. The experiments were carried out in a Vacuum Generators ADES400 photoemission system operating at a base pressure of less than 1×10^{-10} Torr. The energy resolution of the monochromator and energy analyzer were in general chosen to be 0.18 and 0.20 eV, respectively, giving a total energy resolution of about 0.3 eV. The hemispherical electron energy analyzer had an angular resolution of about $\pm2°$. A tungsten grid placed in front of the photoemission system allowed for photon-flux normalization by recording the electron yield from the grid for each photoemission spectrum.

Single crystals of NbC_x were prepared using a vertical floating-zone technique.[16] The composition of the crystals of niobium carbide was determined gravimetrically by ignition in air at 1100 °C of NbC to Nb_2O_5. The composition of the single crystal used in this investigation was $NbC_{0.83}$.

The crystal with orientation (100) was cut by spark erosion and subsequently polished mechanically. It was mounted in the photoemission system with the (100) face perpendicular to the analyzer plane within $\pm2°$ and was cleaned *in situ* by repeated high-temperature flashings to about 1600 °C. The crystal was oriented with the ⟨011⟩ azimuth in the analyzer plane using low-energy electron diffraction (LEED). A sharp 1×1 LEED pattern was observed. The cleanliness of the surface was checked by recording photoemission spectra prior to the actual measurements, and no sign of oxygen or other contaminants could be detected. To maintain a clean surface during the measurements, high-temperature flashings were performed every eighth hour.

In the experimental spectra presented below, the incidence angle of the radiation, θ_i, and the emission angle of the photoelectrons, θ_e, are given relative to the surface normal. The radiation was incident along the ⟨011⟩ azimuth of the crystal at an angle θ_i. In the spectra presented below, all energies are given with respect to the Fermi energy, E_F.

III. RESULTS AND DISCUSSION

A. Band-structure calculation

In order to interpret the photoemission data, a self-consistent band-structure calculation for stoichiometric NbC has been performed using the linear augmented-plane-wave method (LAPW).[17] In the present study the experimental data allow the dispersion of the occupied bands (which are not forbidden by symmetry-selection rules) along the $\Gamma\rightarrow X$ symmetry line to be mapped out. Hence a direct comparison between the experimental results and the theoretically predicted band dispersions can be made. In Fig. 1 the band structure of $NbC_{1.0}$ is shown for energies ranging from -14 to 30 eV. To cover the whole energy range of interest, four different energy regions have been included in the band-structure calculation. The energy parameters E_l, used for the radial wave function inside the atomic spheres, are given in Table I. In the LAPW method[18] the energy eigenvalues are most accurate close to the E_l values and as a rule of thumb the linearization is adequate over an energy range of about 1 Ry. By combining the energy eigenvalues in the four different energy regions the resulting band structure (Fig. 1) was obtained. In the band-structure calculation, 113 unsymmetrized plane waves were used and the first 9 spherical harmonics were included in the expansion of the wave function inside the atomic spheres. A self-consistent potential with an accuracy better than 1 mRy was obtained by using 89 plane waves in the iterations and by calculating the charge density at ten special **k** points in the Brillouin zone.[19] The wave functions of both the core and the valence electrons were recalculated in every iteration cycle and nonspherical contributions to the potential were approximately accounted for by extending the plane waves into the muffin-tin spheres. In the calculations, the local-density functional (LDF) scheme[20] and the Hedin-Lundquist approximation[21] for exchange and correlation have been used. No effort to account for relativistic effects has been made, since, although not negligible in the case of NbC, the difference between nonrelativistic and relativistic energy bands has been shown[10] to be fairly small.

In Fig. 1 the irreducible representations, to which the

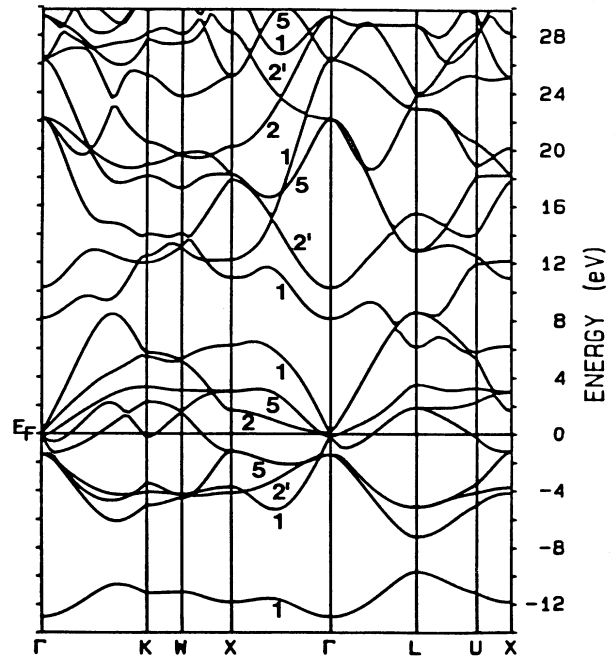

FIG. 1. Calculated band structure of $NbC_{1.0}$ using the LAPW method. The symmetry of the calculated bands is indicated along the $\Gamma\rightarrow X$ symmetry line.

TABLE I. Energy parameters for the LAPW band-structure calculation. For given l value the radial wave functions inside the atomic spheres are expanded around the corresponding energy parameter E_l. The energies (in Rydberg units) are given with respect to the muffin-tin zero (the Fermi energy is located at 0.866 Ry).

Region	l	E_l (C sphere)	l	E_l (Nb sphere)
1	0	0.05	0	0.23
	1	0.56	1	1.90
	2	0.67	2	0.60
	3	0.59	3	0.59
	4	0.57	4	0.46
	5	0.54	5	0.53
	6	0.69	6	0.50
	7	0.57	7	0.58
	8	0.55	8	0.52
2	all $E_l=1.40$, except $E_1^{\mathrm{Nb}}=2.00$			
3	all $E_l=2.40$			
4	all $E_l=3.40$			

calculated bands belong, are indicated along the $\Gamma\rightarrow X$ symmetry line.

B. Experimental results and discussion

It is seen from Fig. 1 that along the $\Gamma\rightarrow X$ symmetry line the valence band of $NbC_{1.0}$ consists of three fully occupied bands of Δ_1, $\Delta_{2'}$, and Δ_5 symmetry. However, at normal emission from the (100) surface of a face-centered-cubic crystal, it has been shown[22,23] that symmetry selection rules forbid initial states of $\Delta_{2'}$ symmetry to be probed. Moreover, initial states of Δ_1 (Δ_5) symmetry can only be excited to an allowed, totally symmetric, final-state band by the perpendicular (parallel) component of the electric field vector. By simple geometrical inspection it is easy to see that the ratio between the perpendicular and the parallel components of the electric field increases monotonically with increasing incidence angle of the radiation, θ_i.

In Fig. 2 experimental angle-resolved photoemission energy distribution curves (EDC's) are shown for photon energies in the range 17–30 eV. The energy-analyzed electrons are emitted in the normal direction and the incidence angle of the radiation is $\theta_i=18°$ in Fig. 2(a) and $\theta_i=45°$ in Fig. 2(b). For convenience, the five structures that are observed in the spectra have been labeled in alphabetical order from the Fermi energy. In Fig. 3 the polarization dependence and energy positions of the experimental peaks are shown in more detail. The two lowest-lying structures, D and E, are seen to gain relative strength as the incidence angle of the radiation increases, indicating emission from initial states of Δ_1 symmetry. Peak E shows strong dispersion with the photon energy; at lower photon energies it moves away from the Fermi energy, exhibits a minimum at about 22 eV, and then shifts back towards the Fermi energy. It also shows strong intensity modulations; a pronounced maximum of the emission intensity is observed around 22 eV, while it becomes considerably weaker at higher photon energies. On the contrary, peak D exhibits no dispersion and gains relative intensity as the energy of the radiation increases. Around -2 eV two structures appear in the experimental spectra. The main one, labeled B, disperses with photon energy and shows a po-

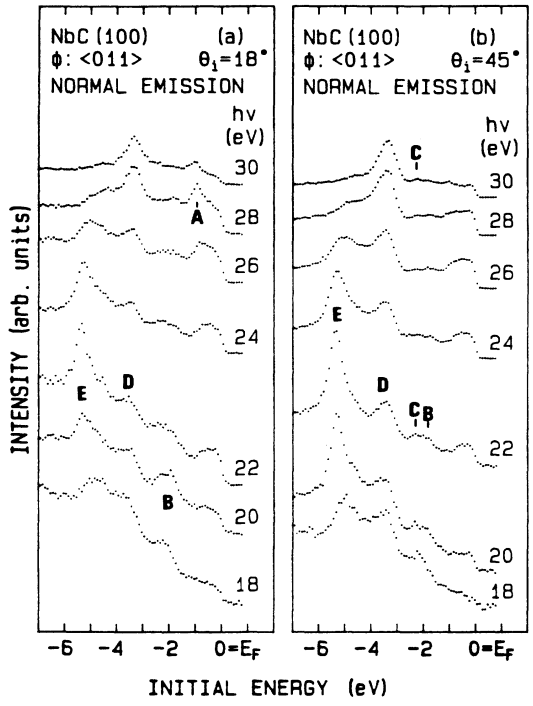

FIG. 2. Angle-resolved EDC's from NbC(100) recorded in the normal-emission direction at various photon energies. The incidence angle of the radiation is (a) $\theta_i=18°$ and (b) $\theta_i=45°$.

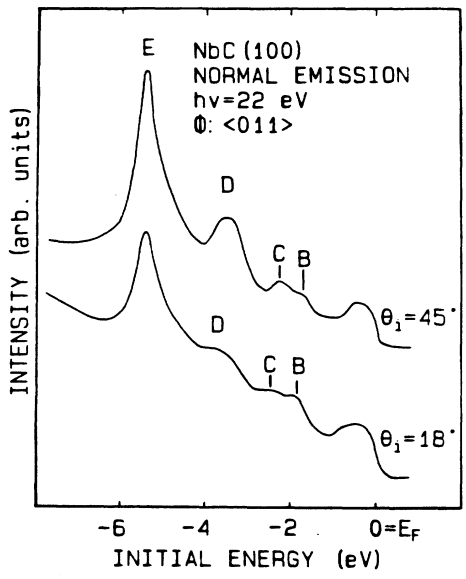

FIG. 3. Comparison of angle-resolved normal-emission EDC's from NbC(100) for 22 eV radiation incident at $\theta_i=18°$ and $\theta_i=45°$.

larization dependence that can be associated with initial states of Δ_5 symmetry. At the larger incidence angle and photon energies above 21 eV, a weak structure *C*, which is located at slightly higher binding energy, can be resolved. We also note that at photon energies above 22 eV and at an incidence angle of $\theta_i = 18°$ a structure *A* appears close to the Fermi energy. It shows no or very little dispersion with the photon energy and seems to be excited preferentially by the parallel component of the electric field.

Since two of the experimental structures show dispersion, one is led to associate them with direct transitions from bulk initial states. In order to confirm this assumption and test the validity of the band-structure calculation, a comparison between the experimental and theoretical band dispersions have been performed. In Fig. 4 the calculated band structure of stoichiometric NbC along the Δ direction is shown together with the experimental results. To obtain the position of the experimental peaks along this symmetry direction, the direct transition model (i.e., transitions that conserve the energy and the reduced wave vector are allowed) and the fact that at normal emission only final states of Δ_1 symmetry can contribute to the photoemission current have been used. The solid circles represent the experimental peaks that can be well explained by the calculated band structure, while the open circles indicate the positions of the features in the experimental spectra that cannot be accounted for by the calculated band structure. For clarity, the calculated final-state band used in the direct-transition model is shown displaced downwards by amounts corresponding to the photon energies 17 and 26 eV. It is seen from Fig. 4 that the flat parts of the Δ_1 and the Δ_5 bands are well reproduced by the experimental results. In this region, there is a fairly good agreement between the experimental and theoretical band dispersions, and the energy positions of the experimental peaks are, in general, located only a few tenths of an electron volt (eV) below the calculated bands. However, the steep part of the Δ_1 band is not reflected by the experimental results; this discrepancy between the experimental and theoretical band dispersions has been observed earlier on transition-metal nitrides[24–26] and can partly be explained by considering the shapes of the bands that are involved in the direct transitions. At these photon energies the final-state band has a slope that is similar to that of the steepest portion of the occupied Δ_1 band. Thus it allows direct transitions to occur over a wide energy range and consequently the emission intensity would be smeared out, prohibiting a sharp peak from being observed in the photoemission spectra. Our photoemission results support this hypothesis; peak *E* exhibits its sharpest structure close to its energy minimum and becomes considerably broader at higher photon energies, reflecting that direct transitions from the steep part of the Δ_1 band start to occur.

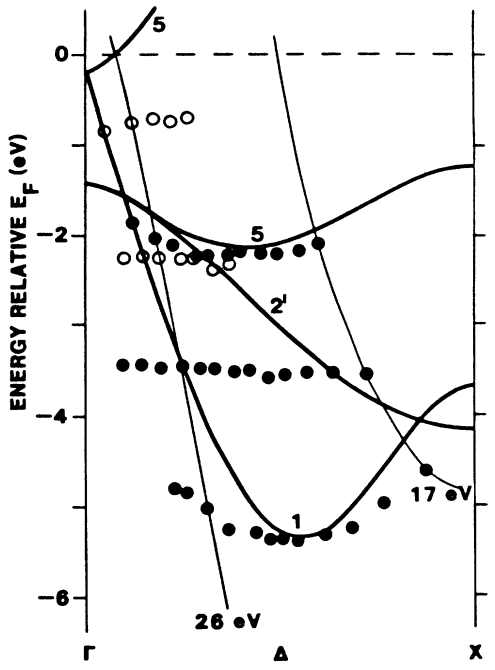

FIG. 4. Comparison between the experimental peak positions using the direct transition model and the calculated energy bands along the Δ symmetry direction. The solid circles represent experimental peaks that can be accounted for by the calculations, while the open circles indicate the positions of experimental features that cannot be explained by the calculated bulk energy-band structure of stoichiometric NbC. In this analysis only the free-electron-like Δ_1 final-state band, located between about 12 and 26 eV (see Fig. 1), has been used. For clarity, this final-state band is shown displaced downwards by amounts corresponding to photon energies of 17 and 26 eV (thin solid lines). See text for details.

Around -3.5 eV, peak *D* in the experimental spectra gives rise to a flat band that does not have a counterpart in the theoretical results. Thus this peak cannot be accounted for by the direct-transition model. Three-dimensional density-of-states (DOS) effects can also be ruled out since off-normal spectra show unambiguously that the energy position of peak *D* is a function of the parallel component of the wave vector; see Fig. 5. The spectra shown in Fig. 5 were recorded at a photon energy of 42 eV but a similar behavior of peak *D* was observed in off-normal spectra recorded at 29 eV. The fact that the energy position of peak *D* almost coincides with the flat part of the Δ_1 band near the *X* point, together with its strong polarization dependence, leads us to believe that it is due to a one-dimensional DOS effect, corresponding to the flat part of the Δ_1 band near the *X* point. Earlier photoemission measurements on nitrides of transition metals[24–25,27] have revealed one-dimensional DOS effects at the Brillouin-zone boundary of the Δ_1 bulk band, and singularities in the one-dimensional DOS are expected to contribute to the photoemission current if phonon-induced effects are not negligible.

So far, we have seen that the three main experimental peaks *B*, *D*, and *E* can be explained satisfactorily by the calculated band structure of stoichiometric NbC. The remaining experimental features, however, cannot be accounted for by the calculations. Although peak *A* ex-

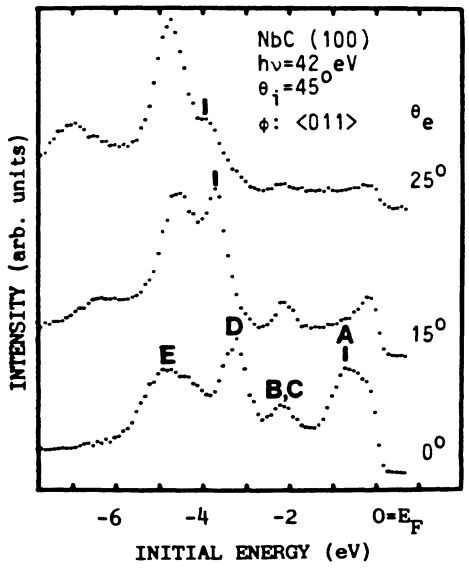

FIG. 5. Angle-resolved EDC's measured at different emission angles θ_e at a photon energy of $h\nu=42$ eV and an incidence angle of $\theta_i=45°$.

hibits a polarization dependence that can be associated with Δ_5 symmetry, it is located in a gap between two bulk bands of Δ_5 symmetry and moreover it shows very little dispersion. It is possible that peak A reflects the Δ_5 bulk band that crosses the Fermi energy, but considering how well the calculated band structure explains the energy positions of peaks B, D, and E, the discrepancy between the experimental results for peak A and the theoretical prediction seems to be too large; the experimental peak positions are located more than 0.6 eV below the calculated band. Hence there are indications that this structure can be related to a surface-induced state. Theoretical studies[12] of the band structure of NbC show that the projected surface Brillouin zone (SBZ) of the (100) face exhibits a band gap near the Γ point along the Σ ($\langle 011 \rangle$) direction. Furthermore, this gap was shown to vanish at about $\frac{1}{3}$ of the Γ-(Σ)-M symmetry line of the SBZ. In Fig. 5 the emission-angle dependence of peak A is illustrated at a photon energy of 42 eV and $\theta_i=45°$. This figure clearly demonstrates that peak A disappears in the off-normal spectra, in agreement with the theoretical predictions.

Previous studies[28–30] on TiN and ZrN have revealed a surface state split off the Δ_5 bulk band and it is plausible that the isoelectronic compound NbC would exhibit similar electronic states. However, in order to verify that this peak is due to a surface-induced state a more careful investigation is required, including gas-adsorption studies and characterization of the state by theoretical models.

Peak C, on the other hand, gains strength by increasing the incidence angle of the radiation (see Fig. 3) and thus cannot be explained on the basis of the bulk energy bands of stoichiometric NbC. However, to this point the vacancy structure of the crystal has not been considered. Since 17% of the sites in the carbon sublattice are unoccupied, one would expect the vacancies to influence the electronic structure of the compound severely. Experimental and theoretical studies[31–37] on the electronic structure of substoichiometric compounds of the refractory carbides and nitrides show that new states are indeed induced by the presence of vacancies. Photoemission experiments in the ultraviolet as well as in the x-ray range have revealed a structure at about 2-eV binding energy, supporting the theoretical predictions. Angle-resolved measurements[24–25] on the (100) face of substoichiometric transition-metal nitrides clearly show that the vacancy state is dominantly excited by the normal component of the electric field. All these findings are in agreement with our experimental results; a nondispersive structure appears in the photoemission spectra at around -2.3 eV with an increased intensity at the larger incidence angle.

The evolution of the experimental EDC's at higher photon energies is shown in Fig. 6. Again, the incidence angle is $\theta_i=18°$ in Fig. 6(a) and $\theta_i=45°$ in Fig. 6(b). Five prominent structures are observed in these spectra. Peak A shows a strong polarization dependence and is clearly discernible at photon energies below around 40 eV and at $\theta_i=18°$. At the higher photon energies, however, a resonant enhancement of the emission intensity close to the Fermi energy is observed, prohibiting peak A from being resolved in the spectra. Peak B is still more pronounced at the smaller incidence angle and exhibits strong intensity variations with photon energy; indeed, its emission intensity seems to be closely related to the resonant enhancement at the Fermi energy. It is also worth noting that peak C is only visible at the lower photon energies, partly due to the enhanced strength of peak B. The two lowest-lying structures, which are believed to originate from a Δ_1 bulk band, show strong dependence on the incidence angle also at these energies. We note that the experimental structures exhibit very little dispersion; the reason for this is at least threefold. Firstly, at these energies there is a lack of suitable final-state bands of Δ_1 symmetry; the final-state band of nearly free-electron character used at the lower photon energies is not available above 27 eV (see Fig. 1). Secondly, at higher energies a larger region of reciprocal space will be sampled by the analyzer, due to its finite acceptance cone. Thirdly, the resonant enhancement at the Fermi energy indicates that other processes start to occur.

Resonant photoemission[38–40] from states just below the Fermi energy have been observed on TiN and ZrN in earlier photoemission experiments.[24–25,41] To date, however, a corresponding resonance for the refractory carbides has not been reported. In accordance with the interpretation for the nitrides, the resonant enhancement is believed to arise from a photon-induced excitation:

$$\text{Nb } 4p^6 4d^4 + h\nu \rightarrow \text{Nb } 4p^5 4d^5 ,$$

followed by the emission of a Nb 4d electron:

$$\text{Nb } 4p^5 4d^5 \rightarrow \text{Nb } 4p^6 4d^3 + e^- ,$$

known as a super-Coster-Kronig decay. Since partial DOS calculations[5] have shown that the states close to

the Fermi energy mainly originate from Nb 4*d* states, photon-induced resonances of this kind would give rise to an enhanced emission intensity at the Fermi level. In order to examine the resonance more carefully, constant-initial-state (CIS) and constant-final-state (CFS) measurements were performed. During the CIS measurements the difference between the photon energy and the kinetic energy of the analyzed electrons was kept constant while scanning the photon energy range of interest. The CFS measurements were performed by keeping the kinetic energy of the analyzed electrons fixed at 3.0 eV, while the photon energy was scanned between 20 and 65 eV. In the present study, the constant parameters were chosen so that the variation with photon energy of the emission intensity close to the Fermi energy (CIS curve) and the absorption of the incident radiation (CFS curve) were measured. In order to normalize out the variation in photon flux, the yield from the beam monitor was used as a reference counter during the measurements, and the curves thus obtained were corrected for variations in the absorption of radiation of the tungsten[42] monitor grid. In Fig. 7 the resulting CIS and CFS curves at an incidence angle of $\theta_i = 45°$ are shown. The binding energy of Nb 4*p* electrons is also indicated. A closer examination of Fig. 7 gives the following. There is a strong resemblance between the CIS and the CFS curve on the low-energy side, indicating that the resonance at the Fermi energy is intimately related to excitation processes involving Nb 4*p* electrons. The CFS curve exhibits two pronounced maxima which are not observed for the CIS curve; in fact the resonance seems to reflect the first structure in the CFS curve. There is a delay of about 10 eV between the maximum of the CIS curve (around 43 eV) and the Nb 4*p* excitation threshold (at about 32.1 and 34.0 eV for Nb $4p_{3/2}$ and Nb $4p_{1/2}$, respectively), in agreement with previous results on transition-metal nitrides.[24–25,41] For comparison, a wide-scan EDC at a photon energy of 58 eV, exhibiting an Auger peak, has also been inserted. The occurrence of an Auger peak at energies above the resonance region shows that there are at least two competitive decay mechanisms for the excited Nb $4p^5 4d^5$ state. When the lifetime of the excited electron $4d^*$ becomes comparable to that of the created 4*p* core hole, the $4d^*$ electron may leak out to the continuum before the $4d \rightarrow 4p$ deexcitation occurs, giving rise to an ordinary Auger decay.

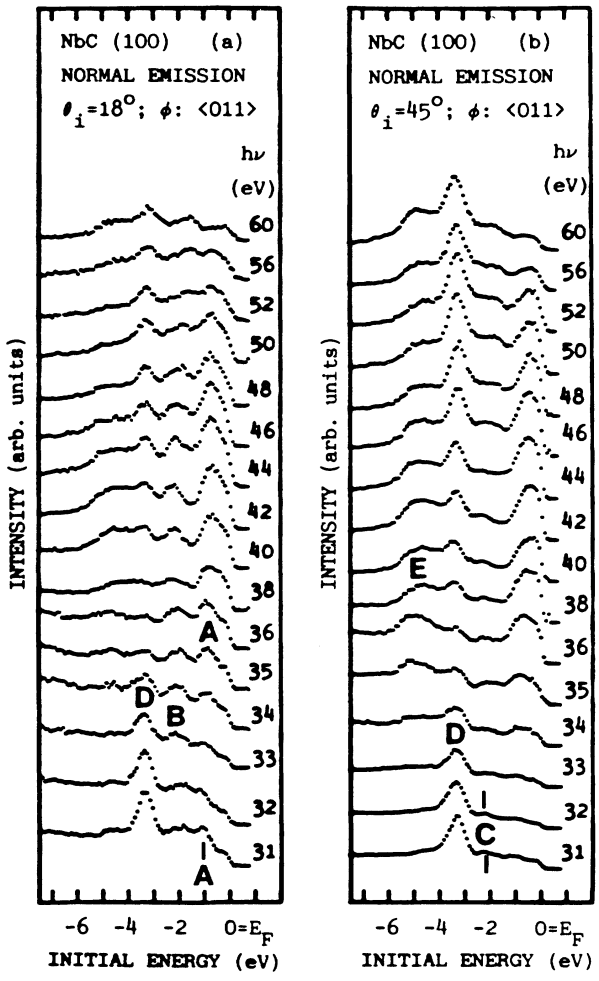

FIG. 6. Angle-resolved EDC's recorded in the normal-emission direction at photon energies above $h\nu = 30$ eV. The incidence angle of the radiation is (a) $\theta_i = 18°$ and (b) $\theta_i = 45°$.

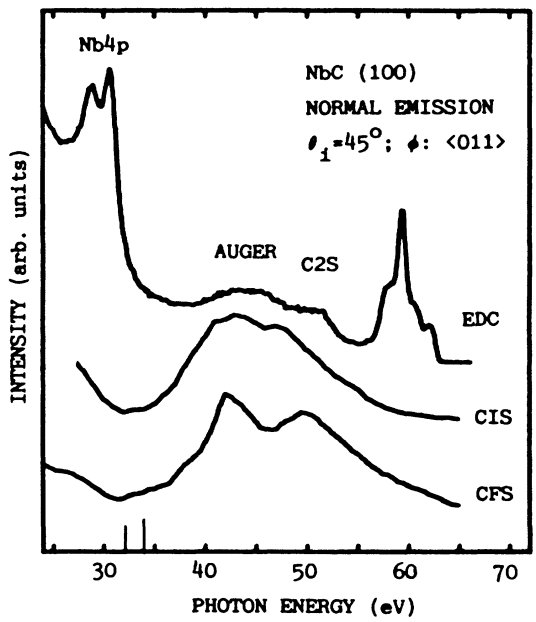

FIG. 7. Comparison between a constant-initial-state (CIS) measurement, corresponding to the variation of the emission intensity at the Fermi energy, and the absorption of radiation as a function of the photon energy, represented by the constant-final-state (CFS) curve. A wide-scan EDC at a photon energy of $h\nu = 58$ eV exhibiting an Auger peak is also shown. The EDC has been shifted arbitrarily so that the width of the Auger peak and the maximum of the CIS curve can easily be compared. The Auger peak is believed to be closely related to the resonance observed at the Fermi energy. The binding energy of Nb 4*p* electrons is indicated by the vertical lines. See text for details.

Hence the width in energy of the Auger peak and the resonance should be qualitatively the same, since they are both determined by the lifetime of the core hole.[40]

All these findings are in agreement with earlier results on TiN(100),[24] indicating that the character of the resonance is essentially the same for compounds containing $3d$ and $4d$ electrons. There are, however, a few differences that should be pointed out. The width of the resonance peak in kinetic energy is considerably larger in the case of NbC, suggesting that the lifetime of the final state is smaller than for TiN in the resonance energy region. Furthermore, as was mentioned above, peak B in the experimental spectra shows a strength that seems to be connected to the resonance at the Fermi energy. In Fig. 8 a comparison between the intensity variation of the structure located around -2.3 eV, which essentially is due to the emission strength of peak B [compare Figs. 6(a) and 6(b)], and the resonance at the Fermi energy is shown as a function of photon energy. This figure illustrates that the emission intensity of peak B reproduces the resonance at the Fermi energy fairly well. Thus the emission strength of peak B is strongly influenced by the onset of Nb $4p$ to Nb $4d$ excitations, which firmly shows that the occupied Δ_5 band has a large amount of Nb $4d$ character.

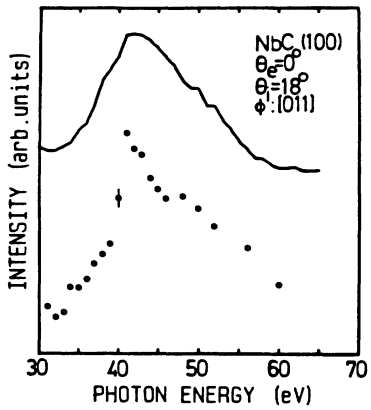

FIG. 8. The photon energy dependence of the emission strength of peak B (solid circles) and the resonant enhancement at the Fermi energy (solid curve). The curves were recorded at normal emission and at an incidence angle of $\theta_i = 18°$. The estimated uncertainty in determining the emission intensity of peak B is indicated by the vertical bar. For clarity, the dotted curve has been magnified by a factor of approximately 6.

IV. SUMMARY

Angle-resolved photoemission energy distribution curves from the (100) surface of $NbC_{0.83}$ have been presented and the normal-emission data have been compared with the results from a band-structure calculation for stoichiometric NbC along the $\Gamma \rightarrow X$ symmetry line. The calculated band structure was found to explain three of the experimental structures very well. Two of these showed dispersion and were interpreted as due to direct transitions from initial bulk energy bands of Δ_1 and Δ_5 symmetry, respectively. A one-dimensional density-of-states feature corresponding to the flat part of the Δ_1 calculated bulk band near the X point was also observed, in accordance with previous results on similar compounds. In the experimental spectra, three features appeared that could not be accounted for by the calculated band structure. One of these was associated with the creation of vacancy-induced states after a comparison with earlier photoemission results and theoretical predictions. A structure that showed strong intensity modulations with the energy and incidence angle of the radiation was found to be located in a symmetry band gap of the calculated bulk-band structure. The possibility that this structure might be due to surface-induced states was suggested in connection with a discussion of its emission-angle dependence and the projected energy-band structure of the surface Brillouin zone. However, to confirm this assignment a more-detailed examination was proposed, since we cannot exclude that this structure might arise from the Δ_5 bulk band that crosses the Fermi level, although the difference between the energy position of the experimental and calculated results seems to be too large.

At the higher photon energies a resonant enhancement of the emission intensity just below the Fermi energy was observed in agreement with previous studies on transition-metal nitrides. The resonance was attributed to a Nb $4p$-to-Nb $4d$ excitation followed by a super-Coster-Kronig decay, leading to an enhancement of the Nb $4d$ photoemission intensity. Finally, a comparison between the intensity variation with photon energy of the two highest-lying structures was made and a striking similarity was observed, showing that for NbC the occupied Δ_5 bulk band is strongly influenced by the Nb $4d$ states.

ACKNOWLEDGMENTS

The authors wish to thank the staff at the Daresbury Synchrotron Radiation Laboratory for their help during the measurements. The financial support from the Swedish Natural Science Research Council is gratefully acknowledged.

[1]L. E. Toth, *Transition Metal Carbides and Nitrides* (Academic, New York, 1971).
[2]M. Cardona and L. Ley, *Photoemission in Solids I* (Springer-Verlag, Berlin, 1978).
[3]J. Redinger, Solid State Commun. **61**, 133 (1987).
[4]J. Redinger and P. Weinberger, Phys. Rev. B **35**, 5652 (1987).
[5]K. Schwarz, J. Phys. C **8**, 809 (1975).
[6]K. Schwarz, J. Phys. C **10**, 197 (1977).
[7]W. E. Pickett, B. M. Klein, and R. Zeller, Phys. Rev. B **34**, 2517 (1986).

[8]G. Ries and H. Winter, J. Phys. F **10**, 1 (1980).
[9]D. J. Chadi and M. L. Cohen, Phys. Rev. B **10**, 496 (1974).
[10]P. Weinberger, Ber. Bunsenges. Phys. Chem. **81**, 804 (1977).
[11]M. Tomasek and S. Pick, Int. J. Quantum Chem. **17**, 1167 (1980).
[12]M. Tomasek, S. Pick, and K. Schwarz, Czech. Chem. Commun. **45**, 1317 (1980).
[13]D. Wesner, S. Krummacher, M. Strongin, R. Carr, T. K. Sham, W. Eberhardt, and S. L. Weng, Phys. Rev. B **30**, 855 (1984).
[14]J. H. Weaver and F. A. Schmidt, Phys. Lett. **77A**, 73 (1980).
[15]H. Höchst, P. Steiner, S. Hüfner, and C. Politis, Z. Phys. B **37**, 27 (1980).
[16]A. N. Christensen, J. Cryst. Growth **33**, 99 (1976).
[17]The computer program used in the band-structure calculation has been developed by S. Persson; see S. Persson, Linköping Studies in Science and Technology, Dissertation No. 147, 1986 (unpublished).
[18]O. K. Andersen, Phys. Rev. B **12**, 3060 (1975).
[19]D. J. Chadi and M. L. Cohen, Phys. Rev. B **8**, 5747 (1973).
[20]P. Hohenberg and W. Kohn, Phys. Rev. **136**, B864 (1964).
[21]L. Hedin and B. I. Lundquist, J. Phys. C **4**, 2064 (1971).
[22]J. Hermanson, Solid State Commun. **22**, 9 (1977).
[23]W. Eberhardt and F. J. Himpsel, Phys. Rev. B **21**, 5572 (1980).
[24]P. A. P. Lindberg, L. I. Johansson, J. B. Lindström, and D. S. L. Law, Phys. Rev. B **36**, 939 (1987).
[25]J. B. Lindström, L. I. Johansson, A. Callenås, D. S. L. Law, and A. N. Christensen, Phys. Rev. B **35**, 7891 (1987).
[26]L. I. Johansson, A. Callenås, P. M. Stefan, A. N. Christensen, and K. Schwarz, Phys. Rev. B **24**, 1883 (1981).
[27]A. Callenås, L. I. Johansson, A. N. Christensen, K. Schwarz, and P. Blaha, Phys. Rev. B **32**, 575 (1985).
[28]A. Callenås, L. I. Johansson, A. N. Christensen, K. Schwarz, P. Blaha, and J. Redinger, Phys. Rev. B **30**, 635 (1984).
[29]L. I. Johansson and A. Callenås, Solid State Commun. **42**, 299 (1982).
[30]A. Callenås and L. I. Johansson, Solid State Commun. **52**, 143 (1984).
[31]H. Höchst, R. D. Bringans, P. Steiner, and Th. Wolf, Phys. Rev. B **25**, 7183 (1982).
[32]L. Porte, Solid State Commun. **50**, 303 (1984).
[33]L. Porte, L. Roux, and J. Hanus, Phys. Rev. B **28**, 3214 (1983).
[34]E. Beauprez, C. F. Hague, J.-M. Mariot, F. Teyssandier, J. Redinger, P. Marksteiner, and P. Weinberger, Phys. Rev. B **34**, 886 (1986).
[35]P. Marksteiner, P. Weinberger, A. Neckel, R. Zeller, and P. H. Dederichs, Phys. Rev. B **33**, 812 (1986).
[36]J. Redinger, P. Weinberger, and A. Neckel, Phys. Rev. B **35**, 5647 (1987).
[37]J. Klima, G. Schadler, P. Weinberger, and A. Neckel, J. Phys. F **15**, 1307 (1985).
[38]S. M. Girvin and D. R. Penn, Phys. Rev. B **22**, 4081 (1980).
[39]L. C. Davis and L. A. Feldkamp, Phys. Rev. Lett. **44**, 673 (1980).
[40]J. A. D. Matthew and S. M. Girvin, Phys. Rev. B **24**, 2249 (1981).
[41]R. D. Bringans and H. Höchst, Phys. Rev. B **30**, 5416 (1984).
[42]R. Haensel, K. Radler, B. Sonntag, and C. Kunz, Solid State Commun. **7**, 1495 (1969).